



RESEARCH ARTICLE

Perturbation in Magnetic Resonance Images from Cerebellum Target Stereotactic Radiosurgery

Kaile Li, PhD ^{a,b,c,*}, Corbin Helis, MD ^c, Esmail Parsai, PhD ^{b,c}, Jeremy Karlin, MD ^c

^a LKL consulting, Hagerstown, MD 21742

^b Decypher, San Antonio, TX 78216

^c Fort Belvoir Community Hospital, Fort Belvoir, VA 22060

* Correspondence: goolkl@gmail.com



PUBLISHED

31 December 2024

CITATION

Li, K., Helis, C., et al., 2024. Perturbation in Magnetic Resonance Images from Cerebellum Target Stereotactic Radiosurgery. Medical Research Archives, [online] 12(12).

<https://doi.org/10.18103/mra.v12i12.6020>

COPYRIGHT

© 2024 European Society of Medicine. This is an open-access article distributed under the terms of the Creative Commons Attribution License, which permits unrestricted use, distribution, and reproduction in any medium, provided the original author and source are credited.

DOI

<https://doi.org/10.18103/mra.v12i12.6020>

ISSN

2375-1924

ABSTRACT

Introduction: Stereotactic Radiosurgery (SRS) is an efficacy procedure in treatment of brain disease. The complicated SRS procedure includes simulation, target definition, treatment planning, target localization and dose delivery. The external accuracy verifications of the whole procedure have been investigated with different quality assurance methodologies. However, the final estimation of SRS procedure should be reflected in the disease lesions inside the patient, and this could be done by employing different imaging modalities at different temporal points, but challenges exist in abstracting the weak signal due to radiation in the images. Therefore, in this study, a method was used to estimate the perturbation information in MRIs at different temporal points after a cerebellum target SRS.

Methods and Materials: A cerebellum target was under an SRS with a single ARC small aperture cone on a Linac machine from Varian Medical system. A series of MRIs in different temporal points have been attained, the temporal range was 0 months, 3 months, 6 months, and 9 months. The volume of interested scans were defined by the isodose volume in the dosimetric plan, which included target volume, and isodose volumes which were at different isodose levels including 100%, 90%, 75%, 60%, 30% and 15% of prescription dose. Through image fusion method, these volumes of interest were defined in the MRIs through the function of copy structures to registered image. Then structure property function to attain the structure statistics including minimum Hounsfield Unit (HU), maximum HU, mean HU, and standard deviation (SD) of HU inside the volume of interest. Vectors were used to represent the separate volumes of interest and corresponding statistics in HU. A relative percentage difference method, which was defined to be the ratio between the differences of SD and mean SD divided by the mean SD to separate the technical variation from imaging procedure.

Result: For the selected volumes of interest, the mean SD HUs were 20.8, 20.4, 24.1, and 26.21 for T1 MRIs, and was 35.2, 17.4, 31.9, and 37.1 for T1 MRIs with contrast. And the least difference in SD HU vector elements was at 3 months, and the average absolute SD HUs was about three in magnitude. Moreover, the relative percentage difference showed a time-spatial vector pattern with special characteristics.

Conclusions: Some significant HU variation can be seen from T1 and T1 with contrast MRIs in temporal and volume discrete matrix. Data analysis could be further improved by eliminating the uncertainty due to technical inconsistency, and similar investigation approach could be applied to the MRIs acquired right after radiation irradiated for SRS.

Keywords: Stereotactic Radiosurgery, MRI, Brain Disease, Perturbation

Introduction

Stereotactic Radiosurgery (SRS) is an efficacy procedure in treatment of brain disease. The radiosurgery was initiated by Leksell gamma procedure [1], and modernized methods have been extended to linear accelerators [2], Cyberknife [3] and so on. The complicated SRS procedure includes simulation, target definition, treatment planning, target localization and dose delivery [4]-[13]. The external accuracy verification of the whole procedure has been investigated with different quality assurance methodologies [5][6]. However, the final estimation of SRS procedure should be reflected in the disease lesions inside the patient, and this could be done by employing different imaging modalities at different temporal points, but challenges exist in abstracting the weak signal due to radiation in the images. The rationale of this philosophy is to mimic the physics study of a few atomic layers of surface morphology between strong Bragg Peaks [14]. More specifically, the perturbation information could be used to estimate and predict the potential abnormal structure at the phases of pretreatment, during treatment and post treatment. Therefore, in this study, a method was used to estimate the perturbation information in MRIs at different temporal points after a cerebellum target SRS,

and the targeting to understand the rationale of radiosurgery in target characteristics, dosimetry accuracy, and radiation dose delivery response and improvement of radiosurgery strategy.

Methods and Materials

This radiosurgery plan was generated in an Eclipse Treatment planning system from Varian medical system. The treatment planning system simulated the x-ray beam, which was generated by a linear accelerator. The simulation included the geometric structure of linear accelerator system and with accurately calibration of dosimetry accuracy. After the dosimetry requirement was given, a dose delivery approach was developed as showed in figure 1. Then patient was treated with high precise setup in the treatment room, and accurate dose was delivered to the intended target. Afterward, different imaging modalities could be employed to trace the treatment outcome.

Firstly, a cerebellum target was under an SRS with a single ARC small aperture cone on a Linac machine from Varian Medical system. The SRS plan is shown in figure 1

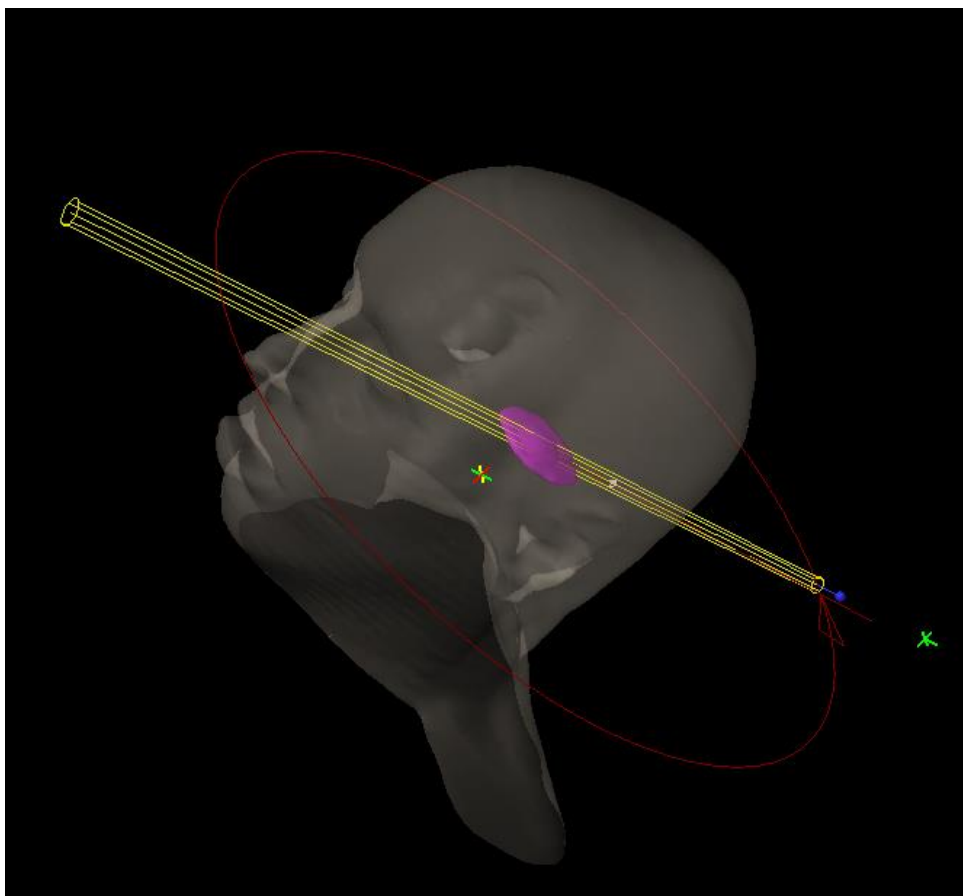


Figure 1: Single ARC Cone plan for SRS.

In this study, a series of MRIs in different temporal points have been attained, the temporal range were 0 months, 3 months, 6 months, and 9 months. The volume of interested scans were defined by the isodose volume in

the dosimetric plan, which included target volume, and isodose volumes which were at different isodose levels including 100%, 90%, 75%, 60%, 30% and 15% of prescription dose, which is shown in figure 2.

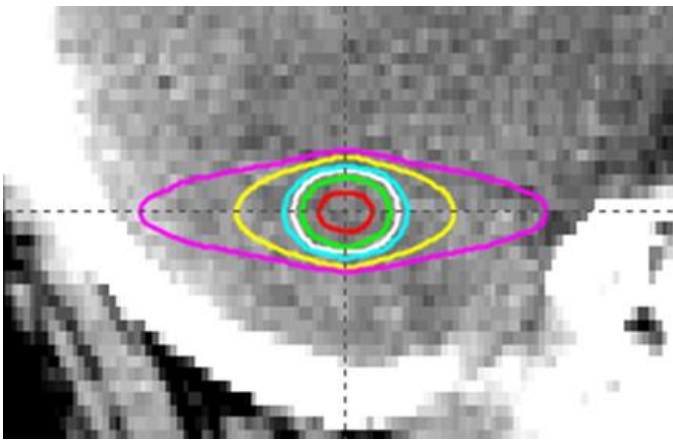
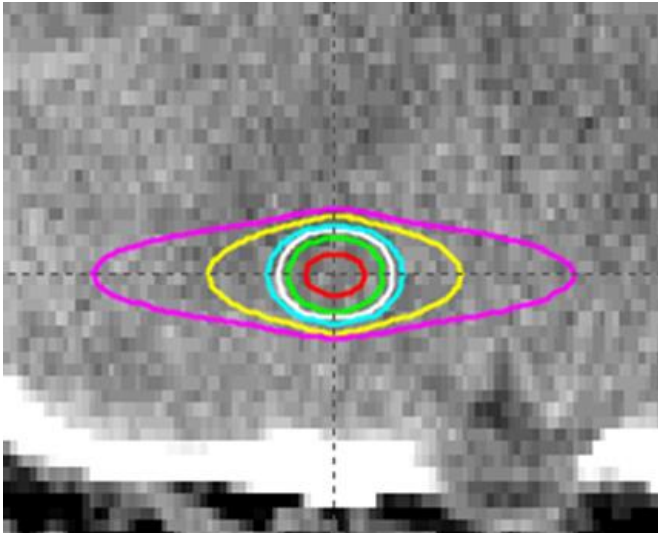
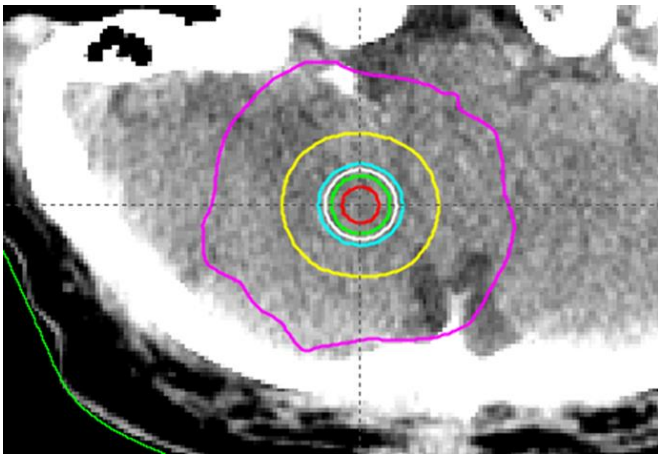


Figure 2: isodose volumes are shown in axial, sagittal and coronal view. Corresponding volumes were 0.04, 0.28, 0.48, 0.77, 2.67, and 10.70cc.

Afterwards, through image fusion method, these volumes of interest were defined in the MRIs through the function of copy structures to registered image. Then structure property function to attain the structure statistics

including minimum Hounsfield Unit (HU), maximum HU, mean HU, and standard deviation (SD) of HU inside the volume of interest (VOI), and this procedure is shown in figure 3.

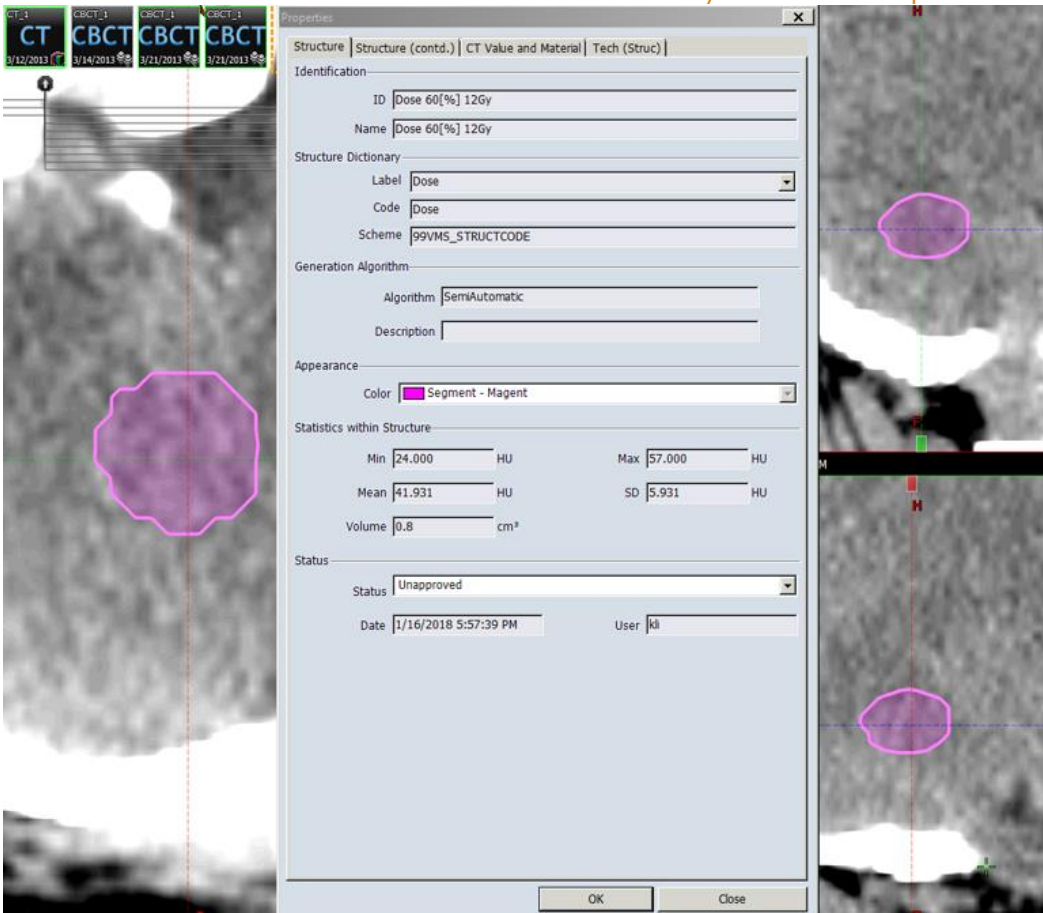


Figure 3: Pixel information of Volume of interest (VOI). It was directly application of the property function of VOI from contouring module from Eclipse Treatment Planning System from Varian Medical System.

Finally, a relative percentage difference method, which was defined to be the ratio between the differences of SD and mean SD divided by the mean SD to separate

the technical variation from imaging procedure. The formula below shows this estimation procedure.

$$\begin{pmatrix} HSD_{V_1} \\ \vdots \\ HSD_{V_N} \end{pmatrix} = \begin{pmatrix} \sqrt{\frac{\sum_{i=1}^{N_{V_1p}} (H_{V_1P_i} - \overline{H_{V_1}})^2}{(N_{V_1p} - 1)}} \\ \vdots \\ \sqrt{\frac{\sum_{i=1}^{N_{V_Np}} (H_{V_NP_i} - \overline{H_{V_N}})^2}{(N_{V_Np} - 1)}} \end{pmatrix}$$

$$SD_{HSD} = \sqrt{\frac{\sum_{i=1}^{N_{HSD}} (HSD_{V_i} - \overline{HSD_V})^2}{(N_{HSD} - 1)}}$$

Note: HSD (HU Standard Deviation in VOI V).
 SD (Standard Deviation).
 N (Number of VOIs or pixels in a VOI)
 P (Pixel in VOI)

Result

For the selected volumes of interest, the mean SD HUs were 20.8, 20.4, 24.1, and 26.21 for T1 MRIs, and was 35.2, 17.4, 31.9, and 37.1 for T1 MRIs with contrast. And the least difference in SD HU vector elements was at 3 months, and the average absolute SD HUs was about three in magnitude. Moreover, the relative percentage difference showed a time-spatial vector pattern with special characteristics. Figure 4 shows some of the analysis. In figure 4(a), the MR T1 with contract image showed a dip in the 3-month time point, and this implied that this imaging setting is sensitive to the treatment lesion response. And in figure 4 (b), the

observation perturbation in formula 1 for surface dose volumes at simulation CT and different MRIs were plotted. The comparison showed the obvious variation happen 15% prescription line, which is 3Gy at this treatment. While considering the actual size of the target, this plot showed the optimal sensitivity volume for analysis in this type of study. Then, as another support of this volume of interest selection, figure 4 (c) was another support for this range of volume of interest by plotting the T1 and T1C SDHU difference, which is the SDHU of T1 MRI subtracting that of the T1 MRI with contract.

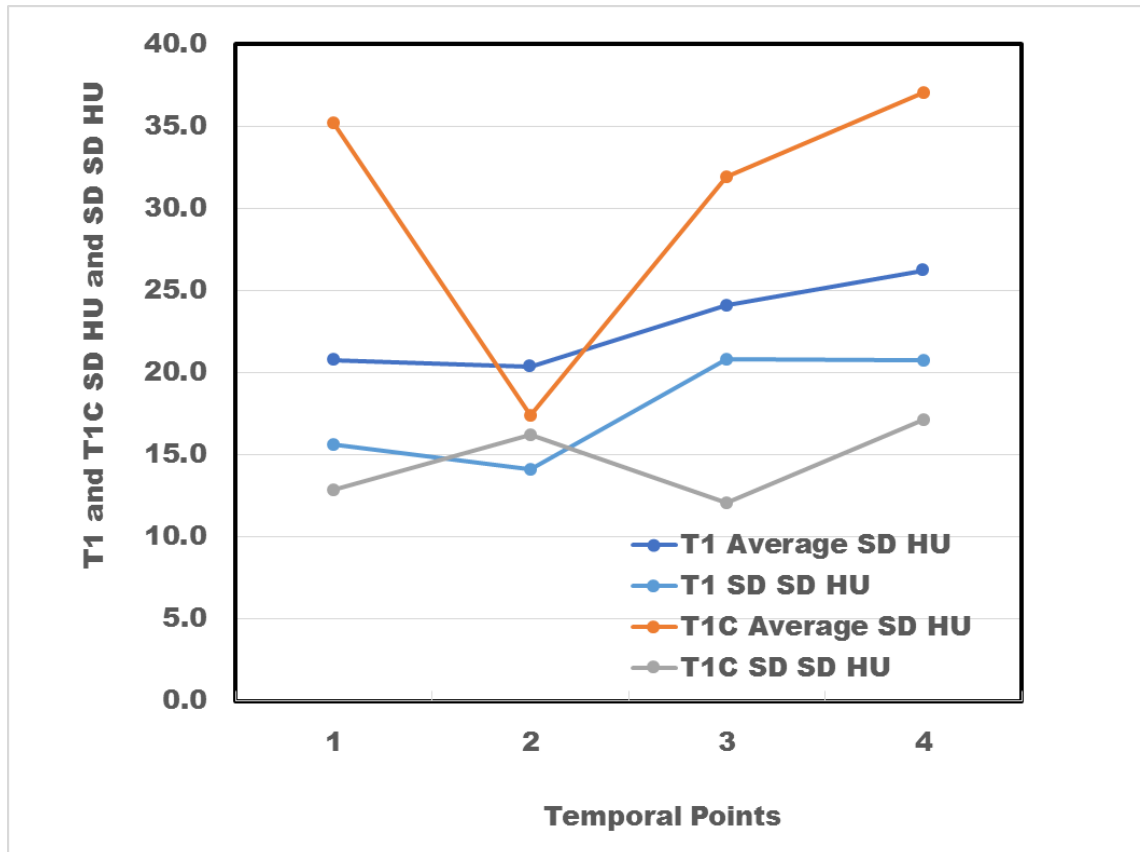


Figure 4 (a): Average standard deviations of HU of T1 images at different temporal points in different VOIs and corresponding SD SD HU.

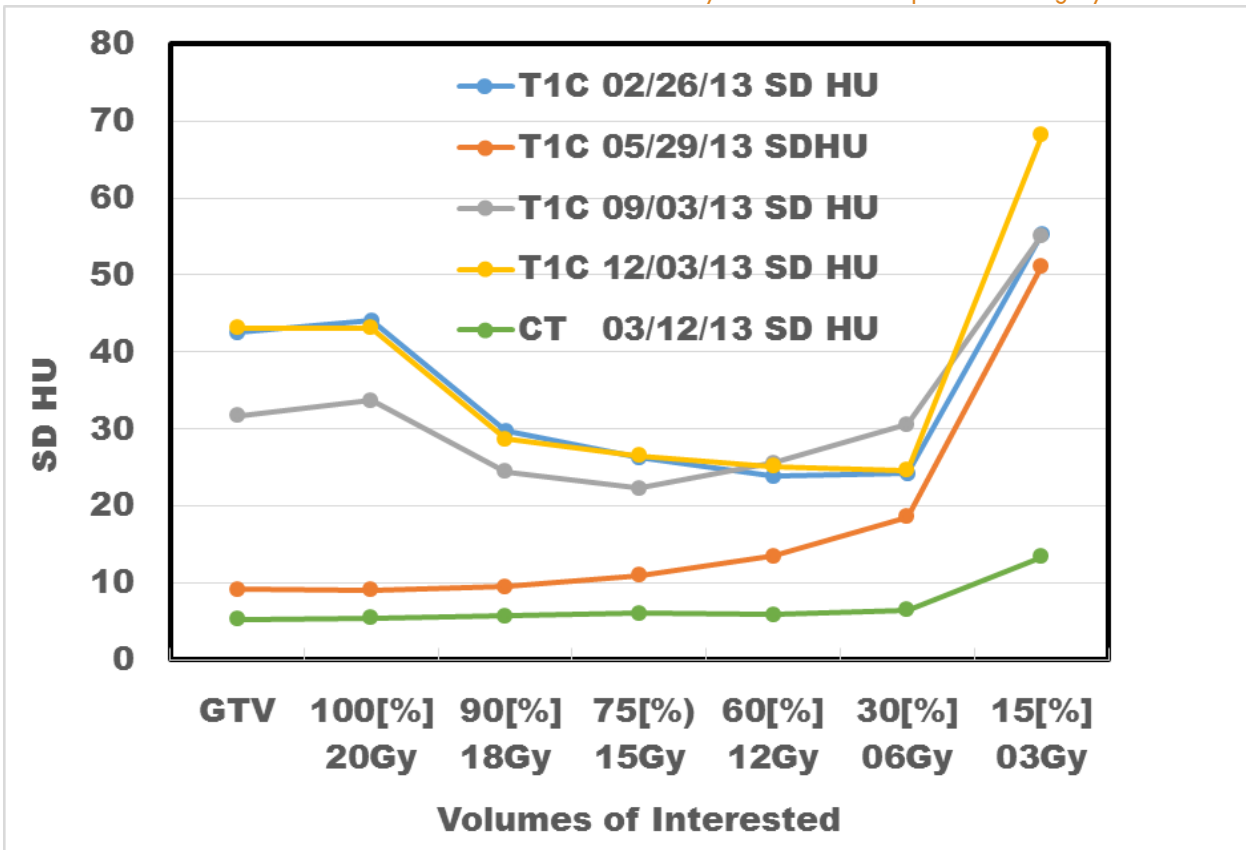


Figure 4 (b): Standard deviations of HU of T1C and plan CT images at different temporal points in different VOIs. It can be seen the significant offsets to the groups at image after 3 months of SRS procedure.

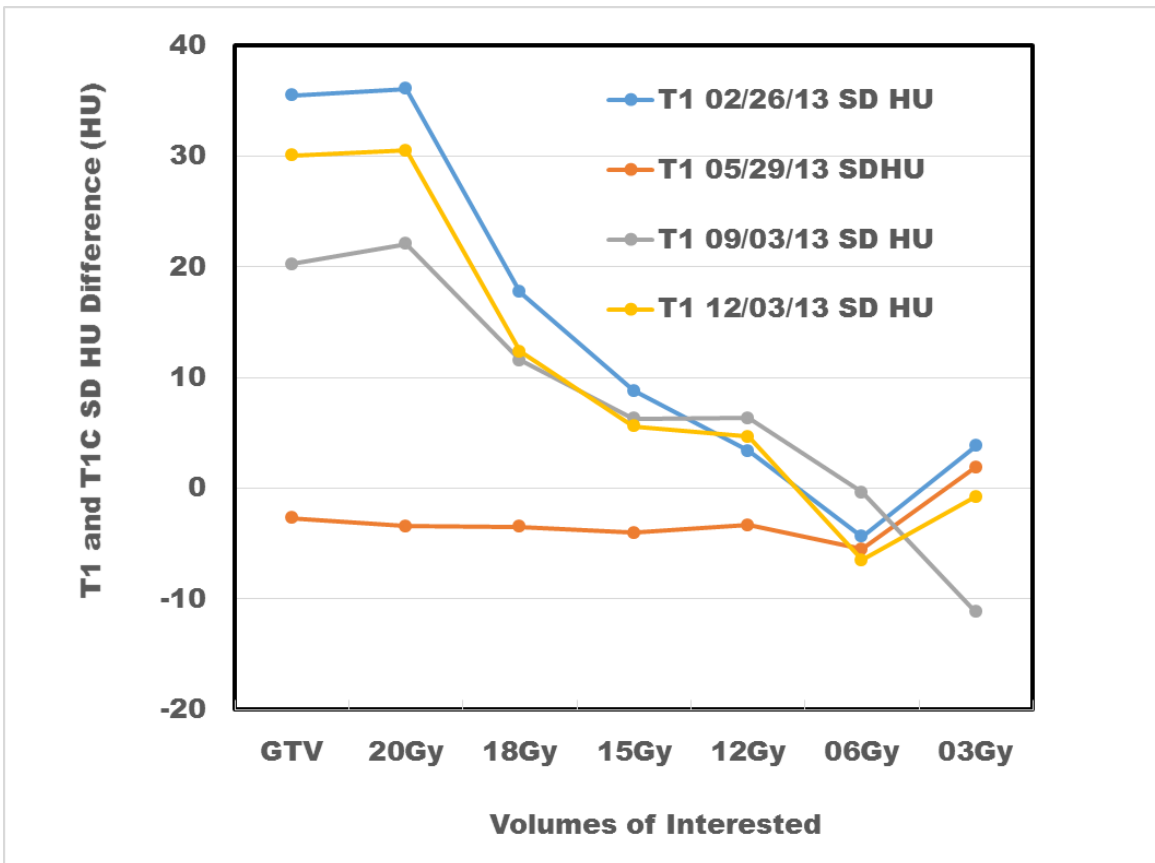


Figure 4 (c): The SD HU variation at between T1 and T1 with contrast MRS was smallest at all the volumes 3 months after SRS procedures. It could imply that the heterogeneity disappeared.

Table 1. T1 and T1 with contrast perturbation for HU standard deviation

Image modality		T1	2/26/13			T1c			
NO.	ROI name	Volume (cc)	SD HU	% /average var HU	relative	SD HU	% /average var HU	relative	T1/T1c SD difference
1	GTV	0.02	7.0603	34%	-66%	42.557	121%	21%	35.4967
2	Dose 100[%] 20Gy	0.02	8.099	39%	-61%	44.175	126%	26%	36.076
3	Dose 90[%] 18Gy	0.11	12.029	58%	-42%	29.772	85%	-15%	17.743
4	Dose 75[%] 15Gy	0.2	17.446	84%	-16%	26.269	75%	-25%	8.823
5	Dose 60[%] 12Gy	0.31	20.626	99%	-1%	23.991	68%	-32%	3.365
6	Dose 30[%] 06Gy	1.75	28.631	138%	38%	24.282	69%	-31%	-4.349
7	Dose 15[%] 03Gy	7.83	51.469	248%	148%	55.281	157%	57%	3.812
average			20.77			35.19			
Image modality		T1	5/29/13			T1c			
NO.	ROI name	Volume (cc)	SD HU	% /average var HU	relative	SD HU	% /average var HU	relative	T1/T1c SD difference
1	GTV	0.02	11.896	58%	-42%	9.199	53%	-47%	-2.697
2	Dose 100[%] 20Gy	0.02	12.569	62%	-38%	9.143	52%	-48%	-3.426
3	Dose 90[%] 18Gy	0.11	12.997	64%	-36%	9.502	55%	-45%	-3.495
4	Dose 75[%] 15Gy	0.19	14.985	74%	-26%	10.963	63%	-37%	-4.022
5	Dose 60[%] 12Gy	0.3	16.826	83%	-17%	13.481	77%	-23%	-3.345
6	Dose 30[%] 06Gy	1.92	24.107	118%	18%	18.609	107%	7%	-5.498
7	Dose 15[%] 03Gy	8.23	49.23	242%	142%	51.113	293%	193%	1.883
average			20.37			17.43			-2.94
Image modality		T1	9/3/13			T1c			
NO.	ROI name	Volume (cc)	SD HU	% /average var HU	relative	SD HU	% /average var HU	relative	T1/T1c SD difference
1	GTV	0.02	11.451	48%	-52%	31.701	99%	-0.8%	20.25
2	Dose 100[%] 20Gy	0.02	11.639	48%	-52%	33.727	106%	6%	22.088
3	Dose 90[%] 18Gy	0.11	12.912	54%	-46%	24.499	77%	-23%	11.587
4	Dose 75[%] 15Gy	0.19	16.051	67%	-33%	22.346	70%	-30%	6.295
5	Dose 60[%] 12Gy	0.3	19.29	80%	-20%	25.621	80%	-20%	6.331
6	Dose 30[%] 06Gy	1.92	31.006	129%	29%	30.614	96%	-4%	-0.392
7	Dose 15[%] 03Gy	8.23	66.259	275%	175%	55.092	172%	72%	-11.167
average			24.09			31.94			
Image modality		T1	12/3/13			T1c			
NO.	ROI name	Volume (cc)	SD HU	% /average var HU	relative	SD HU	% /average var HU	relative	T1/T1c SD difference
1	GTV	0.02	13.108	50%	-50%	43.154	116%	16%	30.046
2	Dose 100[%] 20Gy	0.02	12.607	48%	-52%	43.101	116%	16%	30.494
3	Dose 90[%] 18Gy	0.11	16.358	62%	-38%	28.733	78%	-22%	12.375
4	Dose 75[%] 15Gy	0.19	20.918	80%	-20%	26.518	72%	-28%	5.6
5	Dose 60[%] 12Gy	0.3	20.5	78%	-22%	25.168	68%	-32%	4.668
6	Dose 30[%] 06Gy	1.92	31.101	119%	19%	24.631	66%	-34%	-6.47
7	Dose 15[%] 03Gy	8.23	68.884	263%	163%	68.141	184%	84%	-0.743
average			26.21			37.06			
Image modality		T1	7/24/15			T1c			
NO.	ROI name	Volume (cc)	SD HU	% /average var HU	relative	SD HU	% /average var HU	relative	T1/T1c SD difference
1	GTV	0.02	12.481	44%	-56%	14.648	51%	-49%	2.167
2	Dose 100[%] 20Gy	0.02	12.4	44%	-56%	14.6	51%	-49%	2.2
3	Dose 90[%] 18Gy	0.11	24.32	85%	-15%	20.843	72%	-27%	-3.477
4	Dose 75[%] 15Gy	0.19	29.144	102%	2%	22.957	80%	-19%	-6.187
5	Dose 60[%] 12Gy	0.3	31.467	111%	11%	27.714	96%	-3%	-3.753
6	Dose 30[%] 06Gy	1.92	34.892	123%	23%	30.991	108%	9%	-3.901
7	Dose 15[%] 03Gy	8.23	54.605	192%	92%	69.899	243%	145%	15.294
average			28.47			28.81			
Image modality		T1	1/29/16			T1c			
NO.	ROI name	Volume (cc)	SD HU	% /average var HU	relative	SD HU	% /average var HU	relative	T1/T1c SD difference
1	GTV	0.02	9.595	32%	-68%	43.045	105%	5%	33.45
2	Dose 100[%] 20Gy	0.02	10.432	35%	-65%	42.212	103%	3%	31.78
3	Dose 90[%] 18Gy	0.11	24.789	83%	-17%	34.764	85%	-15%	9.975
4	Dose 75[%] 15Gy	0.19	34.088	114%	14%	36.416	89%	-11%	2.328
5	Dose 60[%] 12Gy	0.3	36.006	120%	20%	37.612	92%	-8%	1.606
6	Dose 30[%] 06Gy	1.92	39.436	132%	32%	36.663	90%	-10%	-2.773
7	Dose 15[%] 03Gy	8.23	55.13	184%	84%	54.914	135%	35%	-0.216
average			29.93			40.80			

Conclusion

In this study, the perturbation philosophy was employed to analyze a temporal series of the MRIs and showed the variation of these perturbation information in response regarding to different volumes of interest in the brain lesion at different dosimetry regions. And the sensitivity of these information was also displayed in different data domains of temporal points. In conclusion, a new outcome analysis tactic was proved to be an effective method for tracing the different abnormal lesions under radiosurgery.

Discussion

As an initial study, some significant HU variation can be seen from T1 and T1 with contrast MRIs in temporal and volume discrete matrix.

For better understanding, data analysis could be further improved by eliminating the uncertainty due to technical inconsistency, for example, figure 5 at right shows the variations when directly applying the “copy structures to

registered image” function, which could be affected by scanning slice thickness, clinician’s judgement on registration, and so on.

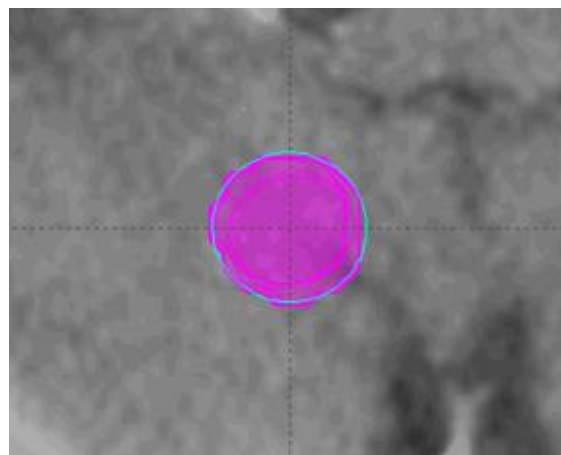


Figure 5: volume variations after directly applying the “copy structure to registered image” function to different temporal point images.

Moreover, similar investigation approach could be applied to the MRIs acquired right after radiation irradiated for SRS.

different physical scales and kinetic response of radiation medicine.

Final, the philosophy of this analysis method could be expanded to different imaging scenarios for objects in

Conflict of Interest: None

References:

1. Leksell L. The stereotaxic method and radiosurgery of the brain. *Acta Chir Scand* 1951; **102**: 316–19
2. W. Lutz, et al, “A system of stereotactic radiosurgery with a linear accelerator”, In. *J. radiat. Oncol. Biol.Phys.* 14, 373, 1988
3. John J. Kresl, Lech Papiez, R.D. Timmerman, James D. Luketich, “Robotic Radiosurgery. Treating Tumors that Move with Respiration”, Springer, 2007
4. Kaile Li, et al, “Aperture Effect for Linac-based SRS in Small Target Treatment”, *Journal of Radiosurgery and SBRT*, vol.4, p21-29, 2016
5. Kaile Li, et al, “Dosimetric Evaluation for Small Target in Linac based Stereotactic Radiosurgery (SRS): Developing a Risk Management Methodology using Perturbation of Localization Technique”, SANTRO, Hangzhou, China, 2010
6. Kaile Li, et al, “Perturbation Analysis of Relationship of Conebeam CT and Stereoscopic Optical Localization System in Frameless Stereotactic Radiosurgery”, ASTRO annual meeting, USA, 2010
7. Kaile Li, et al, “Perturbation of Localization Technique in Dosimetric Evaluation for Small Target in Linac based Stereotactic Radiosurgery (SRS)”, ISRS congress, 2011.
8. Kaile Li, et al, “Improvement of Conformity for Small Target Linac Based Stereotactic Radiosurgery (SRS) By Embedding Machine Geometric Perturbation”, ISRS Congress, 2011
9. Kaile Li, et al, “Comparison of Cone and MLC Linac Based Arc Stereotactic Radiosurgery for Small Target with Different Apertures”, ISRS Congress, 2013
10. Kaile Li, et al, “Strategy of Modality Selection in Linac Based SRS For Multiple Brain Metastatic TARGETS”, ISRS Congress, 2015
11. Kaile Li, et al, “Lucy Phantom Estimation of Geometric Variation for Linac-based Brain Stereotactic Radiosurgery”, ISRS Congress, 2017
12. Kaile Li, et al, “Relationship Between Conformity Indices and Treatment Characteristics in Cone Based Linac Stereotactic Radiosurgery”, AAPM annual meeting, 2015.
13. Kaile Li, et al, “Dosimetric Characteristics of Single Arc Cone and MLC Linac based SRS”, RSS annual meeting, USA, 2017
14. Kaile Li, “Defects at Surface and Interface of Crystals: Theoretical and X-ray Scattering Analysis”, PhD Dissertation, USA 2002